Available online at www.sciencedirect.com
ScienceDirect
Catalysis Today 120 (2007) 399–406
CATALYSIS TODAY
www.elsevier.com/locate/cattod

Hydrogen adsorption characteristics of activated carbon

Hangkyo Jin [a,*], Young Seak Lee [b], Ikpyo Hong [c]

[a] Korea Research Institute of Chemical Technology, P.O. Box 107, Yuseong, Daejeon 305-600, Republic of Korea
[b] Department of Fine Chemical Engineering & Chemistry, Chungnam National University, Daejeon 305-764, Republic of Korea
[c] Research Institute of Industrial Science and Technology, Pohang 790-600, Republic of Korea

Available online 7 November 2006

Abstract

Hydrogen adsorption on activated carbons was investigated in the present works up to 100 bars at 298 K. Coconut-shell was activated by potassium hydroxide, resulting in activated carbons with different porosities. All of prepared activated carbons are microporous and show the same adsorption properties. The complete reversibility and fast kinetics of hydrogen adsorption show that most of adsorbed quantity is due to physical adsorption. A linear relationship between hydrogen adsorption capacity and pressure is obtained for the all samples regardless of their porosities. Hydrogen adsorption capacities are linear function of porosities such as specific surface area, micropore surface area, total pore volume, and micropore volume. The maximum hydrogen adsorption capacity of 0.85 wt.% at 100 bars, 298 K is obtained in these materials.

Keywords: Hydrogen; Storage; Carbon; Adsorption; Porosity

1. Introduction

Hydrogen can play a major role in future energy system. The individual parts of hydrogen energy system such as production, delivery, storage, and conversion are closely interrelated. Among them, hydrogen storage is one of the bottlenecks for the applications in automobile. Several storage methods have been investigated to develop efficient technologies [1].

Hydrogen storage by gas compression, low temperature liquefaction, metal hydride formation, has severe disadvantages. None of the current hydrogen storage technology satisfies all of the needs requested by end users and producers. Many researches are focusing on improving present technologies and searching advanced materials such as adsorbent, absorbent and chemical hydrides. Microporous activated carbons at 77 K seems to be a good candidate for hydrogen storage due to their high porosity and low cost. The hydrogen adsorption process in carbon porous materials at moderate temperature is due to physical adsorption based on van der Waals forces between adsorbent and adsorbate [2,3]. This interaction force is so weak at room temperature that only low adsorption capacity can be obtained [4] and becomes stronger at low temperature, which is proportional to the temperature. Carbon nanotube, carbon nanofiber and activated carbons have attracted lots of interests, however, their hydrogen adsorption capacities scatter over several orders of magnitude [5].

In this work, activated carbons with different porosities have been prepared and investigated as a hydrogen adsorbent up to 100 bars at 298 K to determine further direction to our research on hydrogen storage materials. These activated carbons possess diverse porosities according to their preparation conditions. The hydrogen adsorption capacity is correlated to the porosities of the activated carbons to understand the phenomena of hydrogen adsorption process.

2. Experimental

2.1. Preparation of activated carbon

Various activated carbons are prepared by chemical activation. Coconut-shell was used as a raw material. The elemental analysis of coconut-shell is presented in Table 1. The activating agent was potassium hydroxide. Coconut-shell is crushed up in a particle size smaller than 0.2 mm. Powder raw material was mixed with potassium hydroxide in vibration ball mill. The mixing ratio of raw material and potassium hydroxide

* Corresponding author. Tel.: +82 42 860 7506; fax: +82 42 860 7508.
E-mail address: hkjin@krict.re.kr (H. Jin).

0920-5861/$ – see front matter © 2006 Elsevier B.V. All rights reserved.
doi:10.1016/j.cattod.2006.09.012

Table 1
Elemental analysis for the coconut-shell (wt.%)

C	51.0
H	5.9
N	0.1
O	41.7

ranges from 1:1 to 1:5 in weight. The mixture in the sample holder was heated in a tubular furnace using a heating rate of 5 K min^{-1} up to activation temperature in argon inert atmosphere. The activation was performed for 2 h. The preparation condition is detailed in Table 2. The product was washed with distilled water to remove remaining potassium hydroxide and dried at 423 K for 3 h resulting in activated carbon.

2.2. Pore characterization

The pore structure of activated carbons was characterized by physical adsorption of nitrogen at 77 K in a Micromeritics 2010 apparatus. All the samples were degassed at 623 K for 15 h prior to the measurement.

Nitrogen adsorption isotherms were used for calculating surface area and pore volume through BET equation, *t*-plot, and Gurvitsch rule.

2.3. Hydrogen adsorption

The hydrogen adsorption has been performed by manually controlled high pressure balance, which consists of Rubotherm's magnetic suspension balance and hydrogen boosting system. The resolution of this balance 0.01 mg and working pressure is 150 bars. As it is gravimetric measurement, the apparatus can be used without any severe interference due to temperature deviation. The schematic diagram of hydrogen adsorption apparatus is shown in Fig. 1. Ultra pure hydrogen gas (99.999 wt.%) has been used as an adsorptive and it passed through the oxygen/moisture trap (Phenomenex AG0-4779) which is located just before the adsorption sample to remove trace amounts of moisture and oxygen impurities.

Table 2
Preparation conditions for activated carbons

Sample	KOH/coconut-shell (in wt.)	Activation temperature (K)
AC-1	1	973
AC-2	1	1073
AC-3	1	1173
AC-4	1.5	973
AC-5	1.5	1073
AC-6	2	973
AC-7	2	1073
AC-8	2	1173
AC-9	2.5	973
AC-10	2.5	1073
AC-11	3	973
AC-12	3	1073
AC-13	3	1173
AC-14	3.5	973
AC-15	3.5	1073
AC-16	4	973
AC-17	4	1073
AC-18	4	1173
AC-19	4.5	973
AC-20	4.5	1073
AC-21	4.5	1173
AC-22	5	973
AC-23	5	1073
AC-24	5	1173

A typical hydrogen adsorption experiment using high pressure manual system involved pressurizing a gas reservoir to approximately 120 bars by gas booster. The samples are degassed to eliminate adsorbed gases and water at 373 K for 15 h until pressure and mass did not change for 30 min. Then the desired pressure of hydrogen is introduced into the sample space by opening the valve between the reservoir and the sample space. The pressure, temperature and weight monitored as a function of time. The measured value of balance display is caused by the hydrogen uptake on activated carbon and buoyancy force. As the buoyancy increases according to the increase of adsorption pressure and its effect was larger than the hydrogen uptake, the measured value of balance display decreased in the opposite direction of pressure. The influence of buoyancy can be corrected as follows:

$$M = W \times \left(\frac{1}{(1 - D_{\mathrm{H}})/D_{\mathrm{MA}}} \right)$$

M is the total mass of measurement load, activated carbon and adsorbed hydrogen; W the value of the balance display; D_{H} the density of the hydrogen under measuring room atmosphere; D_{MA} is the density of measuring load including activated carbon.

D_{MA} can be calculated as follows:

$$D_{\mathrm{MA}} = \frac{W_{\mathrm{ML}} + W_{\mathrm{AC}}}{(W_{\mathrm{ML}}/D_{\mathrm{ML}}) + (W_{\mathrm{AC}}/D_{\mathrm{AC}})}$$

W_{ML} is the weight of measuring load; W_{AC} the weight of activated carbon; D_{ML} the density of measuring load, 8.354 g/cm^3; D_{AC} is the density of activated carbon which is measured by pycnometer.

The increase in M is the amount of hydrogen adsorbed. The hydrogen adsorption apparatus was previously tested for leak absence and calibrated with the empty sample cage and well-known carbon standard samples (glassy carbon and MSC-30). Non-porous glassy carbon did not adsorb any noticeable amounts of hydrogen up to 100 bars at 298 K. MSC-30 adsorbed around 0.75 wt.% of hydrogen at 100 bars, 298 K as known.

For this measurement conditions, hydrogen diffusion is so fast that adsorption is almost spontaneous. After no more weight change is detected for 15 min, we get adsorption data. The adsorption temperature, 298 K was kept constant by room temperature control. Buoyancy effect was corrected. Each adsorption test is repeated at different hydrogen pressure from 10 to 100 bars. The mass of the activated carbon samples used for hydrogen adsorption was 500–1000 mg typically.

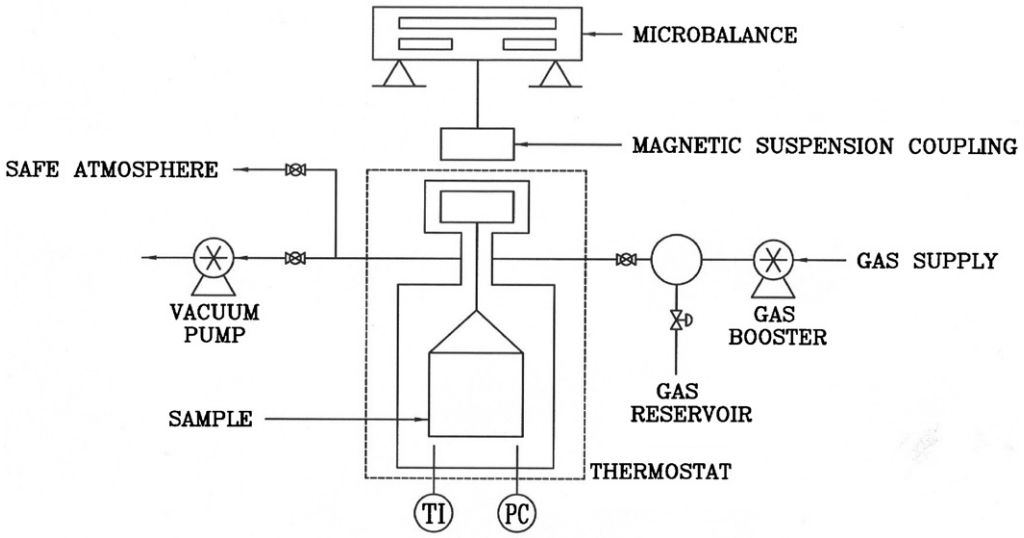

Fig. 1. Hydrogen adsorption apparatus.

3. Results and discussion

3.1. Influence of the activation conditions on porosity

To analyze the influence of activation conditions on porosity, different activation conditions have been used as shown in Table 2. Our previous studies showed that the potassium hydroxide has given an excellent performance as chemical activating agent [6]. It is important to understand that the potassium hydroxide to raw material ratio is the most influencing factor on the porosity of activated carbons. Thus samples AC-1, 4, 6, 9, 11, 14, 16, 19, and 22 have been prepared at the same activating temperature, 973 K. Sample 1 has been prepared with a ratio 1:1 KOH/coconut-shell in weight, whereas in sample 22 the ratio 5:1 KOH/coconut-shell in weight. With these ratios the effect of potassium hydroxide concentration on activation has been studied.

For coconut-shell, the following reaction occurs during dehydration process after KOH impregnation [7],

$$C_nH_xO_y + KOH \rightarrow [C_nH_{x\text{-}1}O_y\text{-}K] + H_2O\uparrow$$

The formation of crossed-linked complexes leads to minimize the formation of tars and other by-products, resulting in a relatively high yield of char.

All of the nitrogen adsorption isotherms are type 1 in spites of different porosities, corresponding to microporous structure [8]. The porosities of activated carbons prepared by potassium hydroxide activation are shown in the following figures.

Fig. 2 shows the effect of KOH/coconut-shell ratio on specific surface area. The specific surface area increased according to KOH/coconut-shell ratio up to 3.5–4.0, then decreased in a similar manner regardless of activation temperature describing parabola shape. Its maximum specific surface area reached up to 2800 m^2/g, which could be used as high performance adsorbent such as gas adsorbent and catalyst support. This highest surface area is close to the maximum theoretical specific surface area of double sided graphite sheet of 2630 m^2/g. It is well known that preparation of activated carbon by potassium hydroxide activation could lead to a very high specific surface area. Such a high specific surface area is due to partial gasification and expansion of gallery height between graphenes through simultaneous intercalation and deintercalation [9–13]. Increasing the temperature from 973 to 1073 K increased the specific surface area, but there was no difference in specific surface area between 1073 and 1173 K.

The *t*-plot can provide the information about the micropore and external surface containing the mesopore and macropore [14]. Fig. 3 shows representative *t*-plots of prepared activated carbons. As the data corresponding to thickness range of

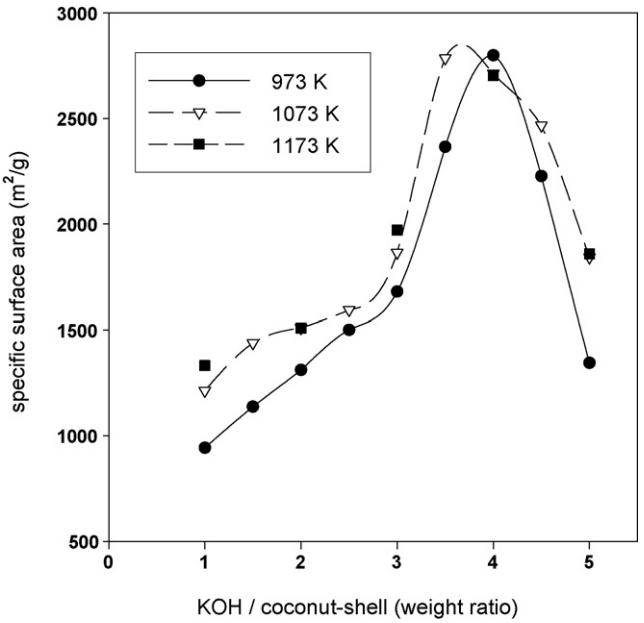

Fig. 2. Effect of KOH concentration on the specific surface area of activated carbon prepared at different activation temperature.

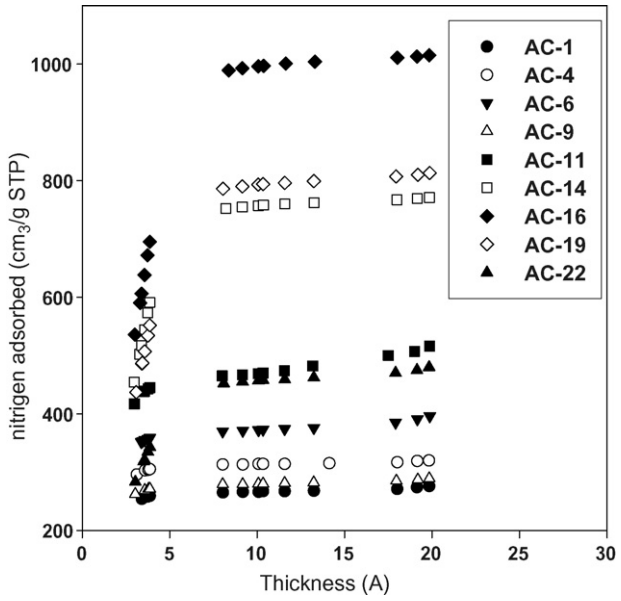

Fig. 3. Representative *t*-plots for nitrogen adsorption at 77 K.

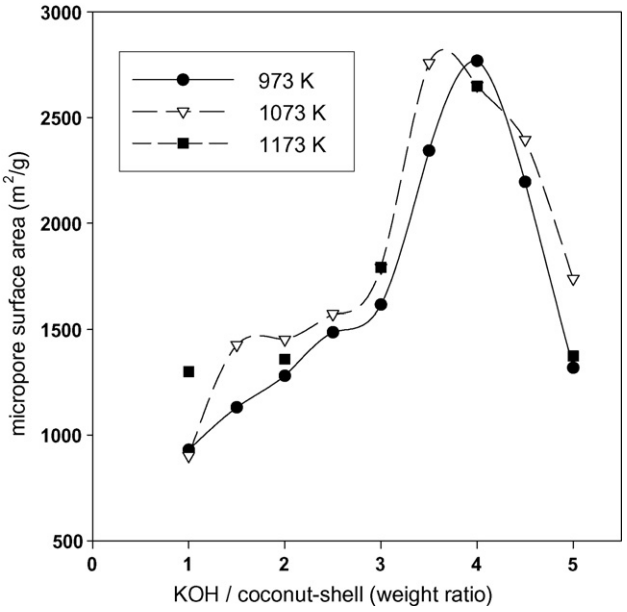

Fig. 5. Effect of KOH concentration on the micropore surface area of activated carbon prepared at different activation temperature.

8–20 Å have shown good linearity, they were fitted to get the slop of linear regression line and the intercept of *Y*-axis.

Fig. 4 shows the effect of KOH/coconut-shell ratio on external surface area. External surface area, corresponding to mesopore area and macropore area, was calculated using the slope of linear regression line of *t*-plot. The external surface area increased according to KOH/coconut-shell ratio and activation temperature, especially drastic at 1173 K. The external surface areas are smaller than specific surface area in general, which is typical in coconut-shell base activated carbon.

Fig. 5 shows the effect of KOH/coconut-shell ratio on micropore surface area, which is calculated by subtracting the external surface area from the specific surface area. The micropore area increased according to KOH/coconut-shell ratio up to 3.5–4.0, then decreased in a similar manner regardless of activation temperature. This progressive KOH concentration rise increased the C-KOH reaction rate, resulting in increasing burn-off. However, for a further KOH concentration increases from 3.5, 4.0 to 5.0, both specific surface area and micropore surface area decreased which may be attributed to excessive carbon burn-off, resulting in the widening of pore diameter and the collapse of some pore walls between pores. It is reported that chemical reactions take place during the chemical activation process as follows. Ehrburger et al. suggested three steps of reaction during the activation process with potassium hydroxide [15].

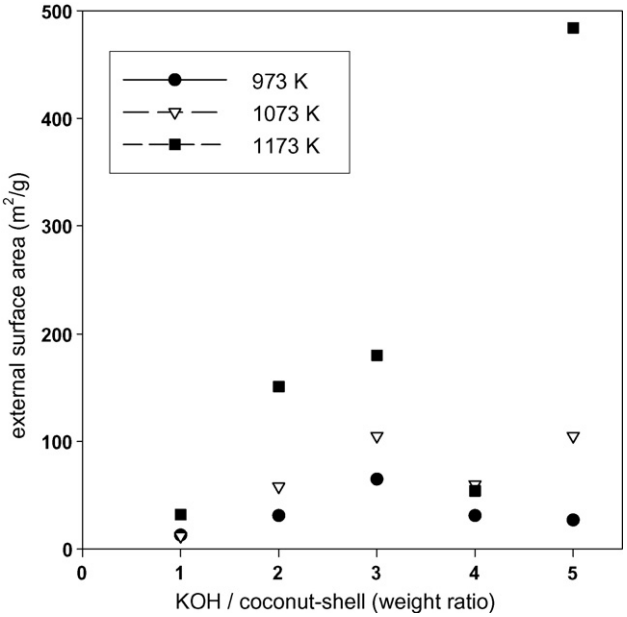

Fig. 4. Effect of KOH concentration on the external surface area of activated carbon prepared at different activation temperature.

1. Formation of potassium carbonate [16]:

$$4KOH + {=}CH_2 \rightarrow K_2CO_3 + K_2O + 3H_2$$

2. Reaction of potassium carbonate with the char close to 750 K, resulting in the formation of carbon dioxide and complex salt (C–O–K) [17].
3. Reaction of potassium carbonate and potassium oxide with carbon above 920 K, resulting in the formation of carbon monoxide [16].

$$K_2O + C \rightarrow 2K + CO$$

$$K_2CO_3 + C \rightarrow 2K + 3CO$$

Otawa et al. suggested that potassium hydroxide may react with precursor through the following 'potassium cycle' in the activation process, resulting in an activated carbon with a very high porosity [18].

1. Dehydration ($KOH \rightarrow K_2O$).
2. Reduction ($K_2O \rightarrow K$).

3. Oxidation ($K \rightarrow K_2O$).
4. Hydration ($K_2O \rightarrow KOH$).

Fig. 5 is similar to Fig. 2 as most of the prepared activated carbons are microporous.

Fig. 6 shows the effect of KOH/coconut-shell ratio on total pore volume. The volume of adsorbed liquid nitrogen at $P/P_0 = 0.997$ divided by it is liquid density gives the total pore volume according to Gurvitsch rule [19]. The total pore volume increased according to KOH/coconut-shell ratio up to 4.0–4.5, then decreased in a similar manner regardless of activation temperature. The total pore volume increased according to the activation temperature from 973 to 1173 K.

Fig. 7 shows the effect of KOH/coconut-shell ratio on micropore volume. The micropore volume is calculated from the *Y*-axis intercept of *t*-plot. Fig. 7 is similar to Fig. 6 as most of the pores in prepared activates carbon are composed of micropore.

Fig. 8 shows the effect of KOH/coconut-shell ratio on external pore volume which composes of mesopore volume and macropore volume. The external pore is calculated by subtracting the micropore volume from the total pore volume. The external surface area increased according to KOH/coconut-shell ratio and activation temperature, especially drastic at 1173 K. The external pore volumes are smaller than micropore volumes in general, which is typical in microporous carbon.

3.2. Influence of porosity on hydrogen adsorption capacity

Fig. 9 shows representative hydrogen adsorption isotherms of prepared activated carbons at 297 K over the hydrogen pressure range 10–100 bars. We have obtained similar shapes of hydrogen adsorption isotherms in spite of their different porosities for all prepared activated carbons. Hydrogen adsorption capacity is a linear function of the pressure, which can be explained with Henry's law. No saturation occurs up to 100 bars and the adsorbed hydrogen layer on the activated carbon surface is very thin. The hydrogen adsorption capacity of the different activated carbons is correlated to their porosities as follows.

Fig. 10 shows the effect of specific surface area on the hydrogen adsorption capacity of the different activated carbons at 100 bars, 298 K. The hydrogen adsorption capacity increases almost linearly according to their specific surface area. In this case the slope of linear regression plot was 2.068×10^{-4} and the *Y*-axis intercept was 0.268. As the specific surface area was calculated from nitrogen adsorption isotherm at 77 K and hydrogen adsorption capacity was calculated from hydrogen adsorption isotherm at 100 bars, 298 K, there were differences in adsorptive, adsorption temperature and adsorption pressure.

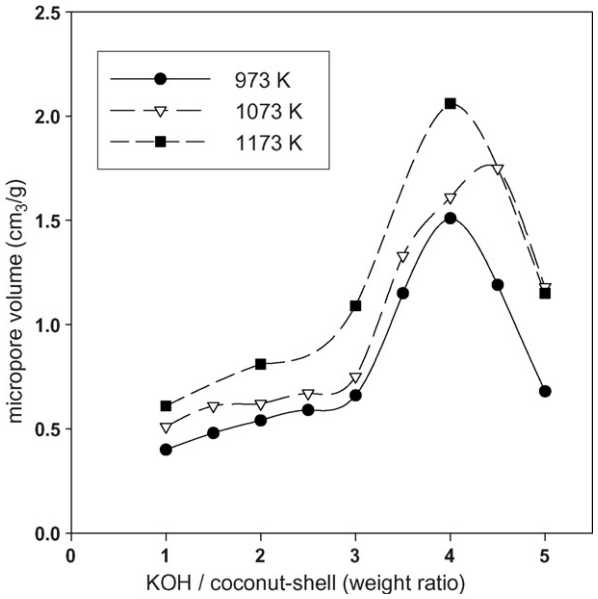

Fig. 7. Effect of KOH concentration on the micropore volume of activated carbon prepared at different activation temperature.

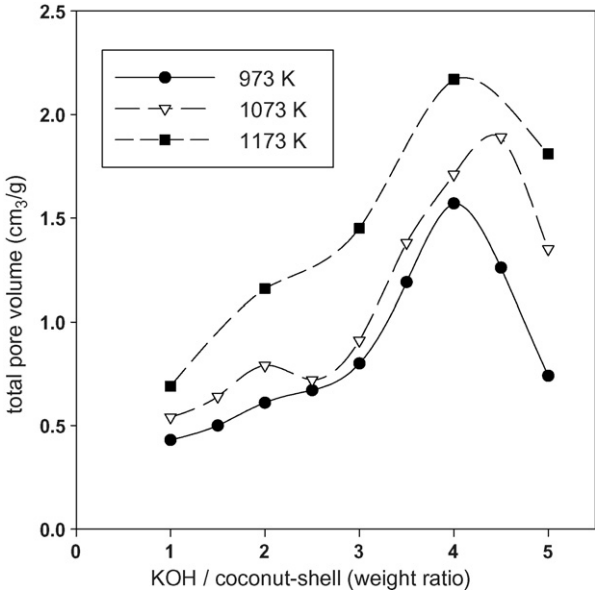

Fig. 6. Effect of KOH concentration on the total pore volume of activated carbon prepared at different activation temperature.

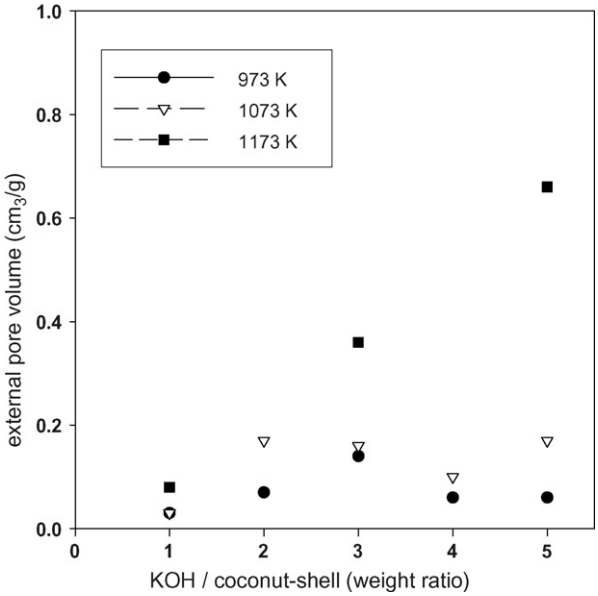

Fig. 8. Effect of KOH concentration on the external pore volume of activated carbon prepared at different activation temperature.

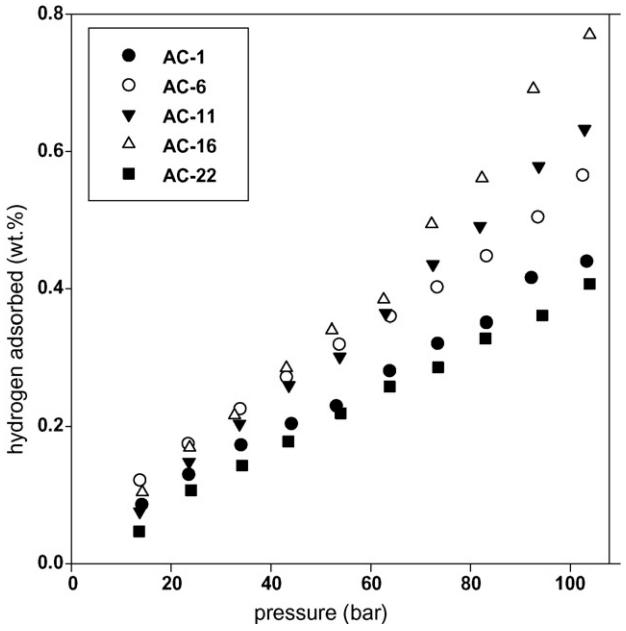

Fig. 9. Representative hydrogen adsorption isotherm of activated carbons at 298 K.

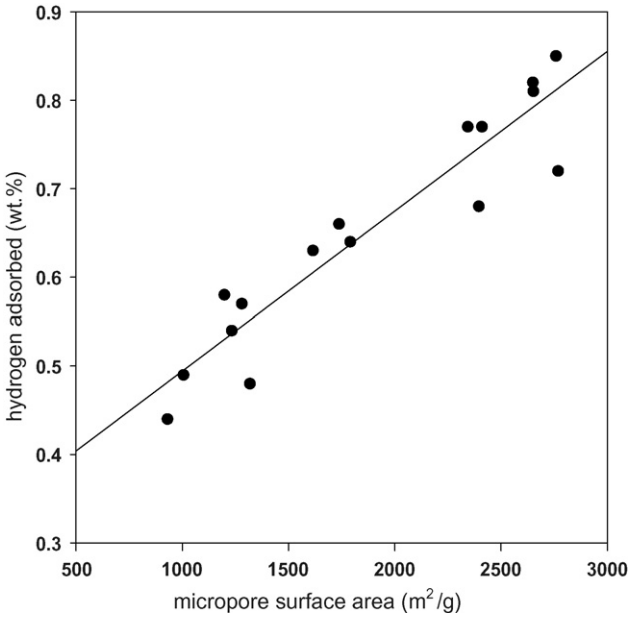

Fig. 11. Effect of micropore surface area on the hydrogen adsorption capacity of activated carbon at 100 bars, 298 K.

It could be thought that the activated diffusion of hydrogen molecules may be possible through very narrow constrictions into cavity, which nitrogen molecules cannot diffuse through. The *Y*-axis intercept in Fig. 10 may be explained due to the activated diffusion.

As shown in Figs. 11–13, the amount of hydrogen adsorption on activated carbon was linearly related to their porosities such as surface area and pore volume. All these results show that the higher the development of porosity, the higher the hydrogen adsorption capacity. It confirms the necessity of using a well-developed microporous carbon material.

The broad range of activated carbons studied in this work and the low hydrogen adsorption capacity dispose us to doubt in large hydrogen storage by activated carbon at room temperature. Hydrogen adsorption measurement seems to be simple, but there are numerous traps to be avoided [20]. The first is that any impurity could increase the weight gain. Moisture drastically increased the weight gain by reaction with the active materials such as alkali species [21]. Other gas impurity could be adsorbed on activated carbon, resulting in incorrect hydrogen adsorption capacity. We used ultra-high pure hydrogen, 99.999% as an adsorptive and attached moisture trap to remove water

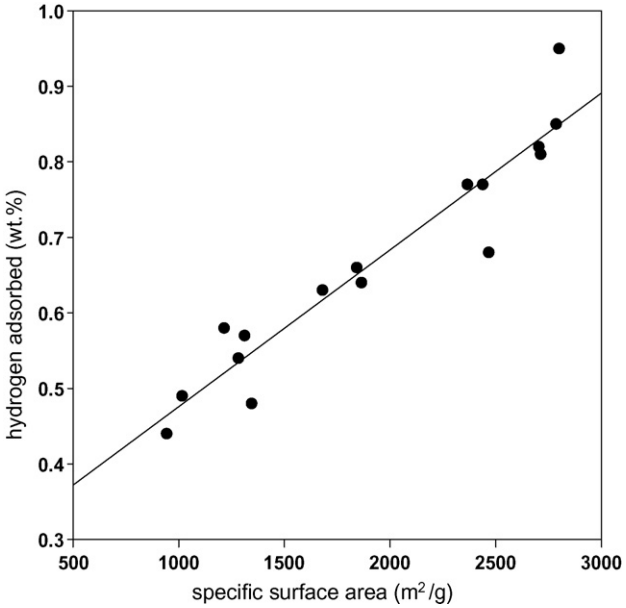

Fig. 10. Effect of specific surface area on the hydrogen adsorption capacity of activated carbon at 100 bars, 298 K.

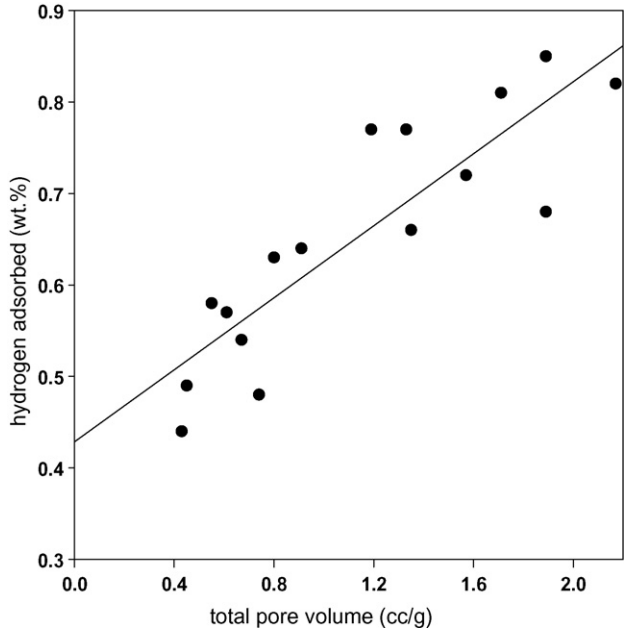

Fig. 12. Effect of total pore volume on the hydrogen adsorption capacity of activated carbon at 100 bars, 298 K.

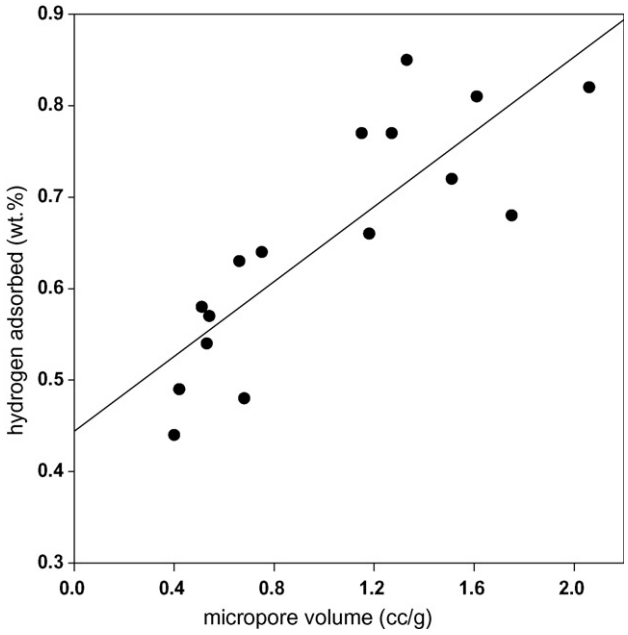

Fig. 13. Effect of micropore volume on the hydrogen adsorption capacity of activated carbon at 100 bars, 298 K.

molecules. The second is the force of buoyancy at high pressure so strong that most of weight change is due to buoyancy force rather than hydrogen adsorption in gravimetric adsorption apparatus. Therefore, the effect of buoyancy was carefully excluded to calculate correct hydrogen adsorption quantities and calibrated with well-known standard samples in this work. The third source of error is that pressure change arising from system temperature variations can incorrectly interpreted as adsorption in volumetric adsorption apparatus. This error effect increases with pressure and may result in several wt.% per degree temperature at 100 bars. The fourth is that it is difficult to distinguish leaks from hydrogen adsorption in volumetric adsorption apparatus. Adsorptive hydrogen gases disappeared from a sample space in both cases. If hydrogen gas leaks from a sample space, it could incorrectly attribute the pressure decrease to hydrogen adsorption. As we used a gravimetric adsorption apparatus, we could avoid the third and the fourth errors. We think that leaks prevention and constant temperature maintenance is important in volumetric adsorption apparatus, and buoyancy effect is carefully calculated in gravimetric adsorption apparatus to get correct hydrogen adsorption quantity. Special caution is needed to remove any impurity from the hydrogen adsorptive and adsorption system.

As AC-15 adsorbs hydrogen five times repeatedly, there are negligible changes in hydrogen adsorption capacities (0.84 ± 0.02 wt.% at 100 bars, 298 K). It shows a complete reversibility of the hydrogen adsorption and the data are sufficiently accurate. When hydrogen gas was introduced into the sample, the equilibrium pressure and weight was reached within a few minutes. This complete reversibility and fast adsorption kinetics indicates that the hydrogen adsorption process on activated carbon is due to physical adsorption.

3.3. Pore filling degree

Table 3 shows the pore filling degree of hydrogen on activated carbons at 100 bars, 298 K. The theoretical hydrogen adsorption capacities amount up to 15 wt.%, however, we have observed a maximum hydrogen adsorption capacity of 0.85 wt.%, very low in pore filling degree, 0.06. The hydrogen adsorption capacity might approach to that of theoretical value by optimizations of adsorption temperature and pressure.

4. Conclusions

This article reports on the chemical activation of coconut-shell with potassium hydroxide and the hydrogen adsorption

Table 3
The pore filling degree of hydrogen on activated carbons at 100 bars, 298 K

Sample	Total pore volume (cm^3/g)[a]	Theoretical hydrogen adsorption capacity (wt.%)[b]	Measured hydrogen adsorption capacity (wt.%)	Pore filling degree[c]
AC-1	0.43	3.01	0.44	0.15
AC-6	0.61	4.27	0.57	0.13
AC-7	0.67	4.69	0.54	0.12
AC-9	0.45	3.15	0.49	0.16
AC-10	0.55	3.85	0.58	0.15
AC-11	0.8	5.60	0.63	0.11
AC-12	0.91	6.37	0.64	0.10
AC-14	1.19	8.33	0.77	0.09
AC-15	1.89	13.23	0.85	0.06
AC-16	1.33	9.31	0.77	0.08
AC-17	1.71	11.97	0.81	0.07
AC-18	2.17	15.19	0.82	0.05
AC-20	1.89	13.23	0.68	0.05
AC-22	0.74	5.18	0.48	0.09
AC-23	1.35	9.45	0.66	0.07

[a] Calculated from liquid nitrogen isotherm at 77 K by Gurvitsch rule.
[b] Calculated from multiplying total pore volume by liquid hydrogen density, 0.07 cm^3/g.
[c] Calculated from dividing measured hydrogen adsorption capacity by theoretical hydrogen adsorption capacity.

characteristics of prepared activated carbons up to 100 bars at 298 K. We have prepared microporous activated carbons with different porosities. The hydrogen adsorption capacities depend almost linearly on porous structure parameters such as specific surface area, micropore surface area, total pore volume and micropore volume. It seems that the promising candidate for hydrogen storage is a well-developed microporous material.

Due to the fast adsorption and desorption kinetics and almost complete reversibility, physical adsorption by activated carbon is a promising methods for hydrogen storage at moderate temperature, however, the highest measured hydrogen adsorption capacity is less than 1 wt.% at 100 bars, 298 K, in spite of their highly developed porosities reaching up to 2800 m^2/g in specific surface area. New materials with ultra-high porosity, even higher than existing activated carbons, should be investigated to achieve sufficient hydrogen storage capacities at room temperature.

Acknowledgement

This research was performed for the Hydrogen Energy R&D Center, one of the 21st Century Frontier R&D Program, funded by the Ministry of Science and Technology of Korea.

References

[1] A. Züttel, Mater. Today 6 (2003) 24.
[2] H.G. Schimmel, G. Nijkamp, G.J. Kearly, A. Rivera, Mater. Sci. Eng. B-Solid 108 (2004) 124.
[3] A. Züttel, P. Sudan, P. Mauron, P. Wenger, Appl. Phys. A 78 (2004) 941.
[4] M. Rzepka, P. Lamp, J. Phys. Chem. B 102 (1998) 10894.
[5] M. Hirscher, M. Becher, J. Nanosci. Nanotech. 3 (2003) 3.
[6] H. Jin, K.S. Yim, Collected Papers of the KHNES Annual Autumn Meeting 2004, 2004, p. 29.
[7] J. Guo, A.C. Lua, J. Colloid Interf. Sci. 254 (2002) 227.
[8] K.S.W. King, D.H. Everett, R.A.W. Haul, L. Moscou, R.A. Pierotti, J. Rouquérol, T. Siemieniewska, Pure Appl. Chem. 57 (1985) 603.
[9] H. Marsh, D.S. Yan, T.M. O'Grady, A. Wennerberg, Carbon 22 (1984) 603.
[10] A. Ahmadpour, D.D. Do, Carbon 34 (1996) 471.
[11] N. Yoshizawa, K. Maruyama, Y. Yamada, E. Ishikawa, M. Kobay-Ashi, Y. Toda, Fuel 81 (2002) 1717.
[12] E. Raymundo-Pinero, P. Azais, D. Cazorla-Amoros, Linares-Solano, K. Szostak, Spanish carbon group, extended abstracts, in: Carbon 2003: International Conference, Oviedo, Spain, July 6–10, 2003 , p. 55.
[13] M.A. Lillo-Rodenas, D. Cazorla-Amoros, A. Linares-Solano, Carbon 41 (2) (2003) 267.
[14] B.C. Lippens, J.H. de Boer, J. Catal. 4 (1965) 319.
[15] P. Ehrburger, A. Addoun, F. Addoun, J.B. Donnet, Fuel 65 (1986) 1447.
[16] Y. Yamashida, K. Ouchi, Carbon 20 (1982) 41.
[17] C.A. Mims, J.K. Pabst, Fuel 62 (1983) 176.
[18] T. Otawa, M. Yamada, R. Tanibata, M. Kawakami, E.F. Vansant, R. Dewolfs, Gas Separat. Technol. (1999) 263.
[19] L. Gurvitsch, J. Chem. Phys. Soc. Russ. 47 (1915) 805.
[20] G.G. Tibbetts, G.P. Meisner, C.H. Olk, Carbon 39 (2001) 2291.
[21] R.T. Yang, Carbon 38 (2000) 623.